A Simple Parcel Theory Model of Downdrafts in Atmospheric Convection

Thomas D. Schanzer

Taste of Research 2021

Supervisor: Prof. Steven Sherwood

School of Physics
Faculty of Science
University of New South Wales
Sydney, Australia

Abstract

Downdrafts are known to play an important role in the dynamics of the Earth's atmosphere and climate, but current quantitative understanding of the mechanisms that generate, maintain and inhibit them is lacking. A simple original model, based on the parcel theory that considers only buoyant forces, is devised to investigate the factors that determine the speed with which a negatively buoyant air mass descends, and the distance it is able to penetrate in the atmosphere. It is found that the evaporation of precipitation is a strong initiating mechanism, that the entrainment of environmental air into a downdraft hinders its descent, and that dryness in the atmosphere above the boundary layer accelerates it, in agreement with the observations and more sophisticated models documented in existing literature.

Acknowledgements

The author is most grateful to his supervisor, Prof. Steven Sherwood, for his patient guidance and mentorship during the ten-week research project whose outcomes are documented in this report. The author also thanks the members of Prof. Sherwood's research group at the UNSW Climate Change Research Centre for some useful suggestions and feedback.

The author would also like to thank the UNSW School of Physics for offering the Taste of Research program under which this project was conducted, and in particular the program coordinator, A. Prof. Sarah Martell. The program has proved to be a very valuable and enjoyable learning opportunity.

Data availability statement

All Python scripts and notebooks used to produce the results in this report are publicly available at `https://github.com/tschanzer/taste-of-research-21T3`.

Notation for thermodynamic variables and constants

p	Total pressure
z	Height
T	Absolute temperature
T_W	Wet bulb temperature
ρ	Density
q	Specific humidity

$q^*(p,T)$	Saturation specific humidity
RH	Relative humidity
$\theta_e(p,T,q)$	Equivalent potential temperature
l	Ratio of liquid water mass to total
λ	Entrainment rate
L_v	Latent heat of vapourisation of water
c_p	Specfic heat at constant pressure of dry air
R	Specific gas constant of dry air
g	Acceleration due to gravity
$(\cdot)_E$	Environmental quantity
$(\cdot)_P$	Parcel quantity

Contents

1 Introduction and theory

Along with updrafts, downdrafts—downward-moving masses of air—are important features in the dynamics of the Earth's atmosphere; they transport mass, momentum, heat and moisture vertically and also generate and maintain storms (Knupp and Cotton 1985).

Indeed, one of the main objectives of present-day research into downdraft dynamics is to improve the predictions of global climate models (Thayer-Calder 2013), whose output informs the understanding of the larger-scale dynamics, including the pressing issue of anthropogenic climate change. Specifically, the high computational cost of running a global climate model over the necessarily large spatial domain and prediction timescales constrains their maximum resolution, which is still too coarse to describe convection. The models therefore employ schemes known as *parametrisations* which estimate the effect of convection on the state of the model using the information available at each time step; an accurate estimation requires a strong understanding of the factors that govern convection.

On a smaller scale, strong downdrafts that reach the Earth's surface (*downbursts*) are known to cause significant damage to man-made structures and create hazardous, or even deadly, conditions for aircraft (Thayer-Calder 2013). Another aim of downdraft research is therefore to understand the mechanisms that generate such extreme events and improve the ability to predict them in advance.

Considering these motivations, the goal of this work is to gain insight into which processes and conditions initiate, and which maintain or inhibit, downdrafts. The approach will be to construct a significantly simplified model of a downdraft using *parcel theory*.

An air parcel is a mass of air with an imaginary flexible (but usually closed) boundary; under the usual assumptions, its exact size and shape are irrelevant. The only force assumed to act on the parcel is the net buoyant force (per unit mass), given in accordance with Archimedes' principle by

$$b = \frac{\rho_E - \rho_P}{\rho_P} g. \tag{1}$$

If the parcel is lowered in the atmosphere to a location with a higher pressure, the work done to compress it and any heat exchanged will manifest as a change in its internal energy in accordance with the first law of thermodynamics. The second key assumption of parcel theory is that this process is adiabatic; this is valid due to the low thermal conductivity of air.

The potential presence of water in gas, liquid and solid phases in the parcel is a major complication; under the assumption that the parcel remains in phase equilibrium (i.e., changes are slow enough for excess liquid to evaporate if the vapour pressure is below the saturation value), there are two modes of adiabatic descent the parcel may undergo. If no liquid is present, the descent is *dry adiabatic* and the rate of work on the parcel causes it to warm at an approximate rate of $9.8\,\mathrm{K\,km^{-1}}$. If liquid is present, the descent is *moist adiabatic*: progressive warming of the parcel raises its saturation vapour pressure, allowing the liquid to progressively evaporate during descent, with the necessary transfer

of latent heat from the air to the water creating an opposing cooling effect.

Moist adiabatic descent is commonly assumed to be either *pseudoadiabatic*, in which case liquid water does not contribute to the heat capacity of the parcel (as if it precipitates from the parcel immediately upon condensation), or *reversible*, in which case the liquid does contribute to the heat capacity. A reversibly descending parcel warms at a slightly slower rate than a pseudoadiabatically descending one due to its larger heat capacity Saunders (1957). Both modes were investigated, but reversible descent was ultimately chosen as it is the more realistic case for a parcel known to retain liquid water.

If the pressure and temperature of the parcel are thus known at any point in its descent, its density may be calculated using the ideal gas law,

$$\rho = \frac{p}{RT_v}, \tag{2}$$

where T_v is the *virtual temperature* that contains a small correction to account for the different density of water vapour. If an mass l of liquid water, per unit total parcel mass, is also present, it is easily shown that (assuming the liquid occupies negligible volume) the corrected parcel density is

$$\rho = \frac{p}{RT_v(1-l)}. \tag{3}$$

Knowledge of the parcel and environmental densities enable calculation of the buoyant force per unit mass on the parcel using (1), and its resulting displacement and velocity may be obtained by (numerically) solving the ODE

$$\frac{\mathrm{d}^2 z}{\mathrm{d}t^2} = b(z). \tag{4}$$

2 Literature review

In their review of existing literature, Knupp and Cotton (1985) identify four downdraft types based on the mechanisms that generate or maintain them, which informed the methods of this investigation: penetrative, cloud-edge, overshooting and precipitation-associated. The penetrative type arises when subsaturated environmental air is *entrained* (mixed) into saturated cloudy air, allowing evaporation of the excess liquid that creates negative buoyancy. The cloud-edge type, they note, is less understood and may result from evaporative cooling at the edges of clouds. An overshooting downdraft may be generated when the inertia of an updraft causes it to rise beyond its level of neutral buoyancy and subsequently sink. The precipitation-associated downdraft is generated by the evaporation of precipitation into subsaturated air beneath a cloud, with the cooling creating negative buoyancy. They note that $20\,\mathrm{m\,s^{-1}}$ is a typical upper limit on downdraft velocity in all cases. The model presented in this work most closely describes the precipitation-assiciated and penetrative types.

Knupp and Cotton (1985) find that downdrafts often become subsaturated during descent, a conclusion reproduced by Thayer-Calder (2013) in a Lagrangian (parcel-tracking) study of the output of a cloud-resolving model. The latter also found that downdrafts often descend past their neutral buoyancy levels. These findings are clearly reproduced in this work.

Market et al. (2017) use case studies to investigate the dependence of downdraft penetration depth on quantities known as *downdraft convective available potential energy* (DCAPE) and *downdraft convective inhibition* (DCIN). The former is a measure of the maximum kinetic energy per unit mass a parcel in a given environment may gain, and the latter is a measure of the work necessary to bring the parcel to the ground once it passes its neutral buoyancy level, against the upward buoyant force. Both are calculated as integrals of the buoyant force with respect to height between chosen initial and final levels (bracketing regions of positive buoyancy for DCAPE and negative buoyancy for DCIN). They come to the conclusion that the smaller the DCIN relative to the DCAPE, the more likely downdrafts are to penetrate stable parts of the atmosphere and reach the ground. Sumrall (2020) conducts further case study investigations, with findings supporting a hypothesis that small ratios of |DCIN/DCAPE| are correlated with stronger and deeper downdraft activity and surface winds, and vice versa for large ratios. This work also reproduces the above findings.

3 Methods

3.1 General approach and code structure

All calculations were performed in Python 3.8.5. Other than basic thermodynamic calculations (such as saturation specific humidity from pressure and temperature, and density according to (2)) which were imported from the open-source `MetPy` package (May et al. 2021), the model was built from scratch and from first principles. The model is divided between three scripts, whose functions are described below.

`environment.py` defines the `Environment` class, which provides utilities for finding the various environmental variables at any height, allowing the model to be applicable to any real or idealised atmospheric *sounding* (vertical profile of environmental variables). The class is instantiated by supplying discrete vertical profiles of pressure, temperature and dewpoint, and the resulting instance offers methods that interpolate the data and calculate derived quantities at any height. For example, the density at 5 km in an `Environment` named `sydney`, initialised with a measured sounding over Sydney, is given by `sydney.density(5*units.kilometer)`.

`thermo.py` provides various thermodynamic calculations that are not available in `MetPy`. The following important functions are implementations of existing published methods:

- *Equivalent potential temperature* (a variable with dimensions of temperature that is conserved during moist adiabatic descent) as a function of pressure, temperature and specific humidity, following the empirical formula presented by Bolton (1980) in his Equation (39),
- DCAPE and DCIN for a given atmospheric sounding, following the definitions of Market et al. (2017),
- The exact analytical solution for the *lifting condensation level* (LCL), the pressure level to which a parcel must be lifted in order to cool it to the point of saturation and the temperature at this point, adapting the implementation of Romps (2017),
- The *wet bulb temperature* (the temperature to which a parcel is cooled by evaporation of water to the point of saturation, at constant pressure), using Normand's rule. Normand's rule states that if a parcel is lifted dry adiabaically to its LCL (which we find using the method of Romps (2017)) and lowered moist adiabatically back to the initial level, it attains its wet bulb temperature.
- An approximate, but faster, wet bulb temperature calculation implementing the method of Davies-Jones (2008), and
- The parcel temperature resulting from reversible adiabatic ascent or descent, implementing a numerical solution of Equation (3) presented by Saunders (1957).

Additional original functions written for the model are described in the subsections that follow.

`entraining_parcel.py` defines the `EntrainingParcel` class, which assembles the functions of the other two scripts to create the final model. It is instantiated by supplying an `Environment` instance and offers methods for calculating parcel displacement and velocity as functions of time, given some initial conditions, on that atmospheric sounding. These are described in detail in the following subsections.

3.2 Temperature of an entraining, descending parcel

The theory of the model developed in this work is a generalisation of the standard parcel theory in that it accounts for a parcel that continually entrain air from its environment, exchanging heat and liquid and/or gaseous water. Following the generally accepted pattern common to the approaches documented by Knupp and Cotton (1985), the cumulative mass exchanged by entrainment is assumed to be a linear function of distance descended, with the constant of proportionality λ termed the *entrainment rate*. The dimension of λ is inverse length; for a parcel of mass m, the total mass exchanged after it descends a distance Δz is $m\lambda\Delta z$. One of the main contributions of this work is to develop a method for calculating the temperature of a parcel that simultaneously descends and entrains in

this manner. The general approach is to divide the descent into small vertical steps, each one consisting of a discrete entrainment process and a short adiabatic descent.

Mixing and phase equilibration

The first step towards finding the temperature of an entraining and descending parcel is to find the state that results from a discrete entrainment step, without descent. The procedure is depicted in Figure 1 and is based on the conservation of total enthalpy and water mass, and the requirement that the parcel return to phase equilibrium after its exchange with the environment (by either condensing or evaporating water). In the cases where evaporation or condensation is necessary, we recognise that the resulting temperature is the parcel's wet bulb temperature.

Dry and/or reversible moist adiabatic descent

After the parcel has mixed with the environment and returned to phase equilibrium, it descends adiabatically. The central complication in this step is that the descent may be dry (if no liquid water is present in the parcel), moist (if liquid water is present), or part moist followed by part dry (if the small amount of liquid water present fully evaporates midway during descent). If this third case is necessary, the final temperature may be computed by recognising that the parcel conserves its equivalent potential temperature, and therefore finding the unique final temperature that satisfies this requirement using numerical root-finding. Figure 2 shows all the steps involved.

Finding temperature as a function of height

The previous two procedures, performed one after the other, give the state of the parcel after a small discrete downward step. A calculation that is valid over larger distances must divide the vertical interval into small steps (50 m was found to give sufficient convergence by trial and error) and repeat the discrete method at each one until the desired final height is reached. This process is depicted in Figure 3.

3.3 Density, buoyancy and motion of a descending parcel

Now, knowing the temperature of the parcel as a function of height/pressure, it is a relatively simple matter to find its density using (2) and the buoyant force per unit mass acting on it using (1). We then numerically solve (4), expressed as the first-order system

$$\frac{\mathrm{d}}{\mathrm{d}t}\begin{pmatrix} z \\ w \end{pmatrix} = \begin{pmatrix} w \\ b(z) \end{pmatrix}.$$

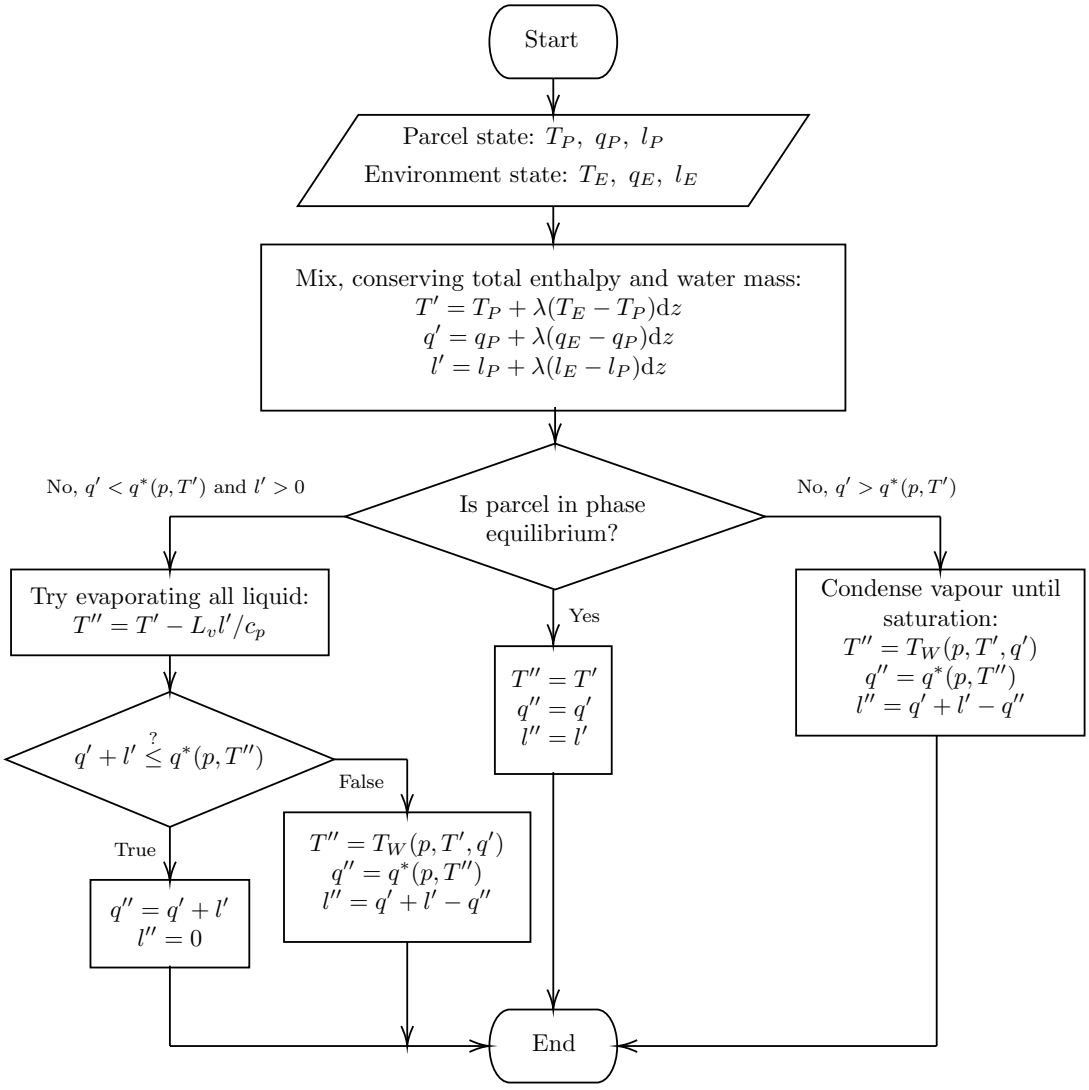

Figure 1: Flowchart for the mixing and phase equilibration calculation (functions `mix` and `equilibrate`) performed at each downward step for the entraining downdraft.

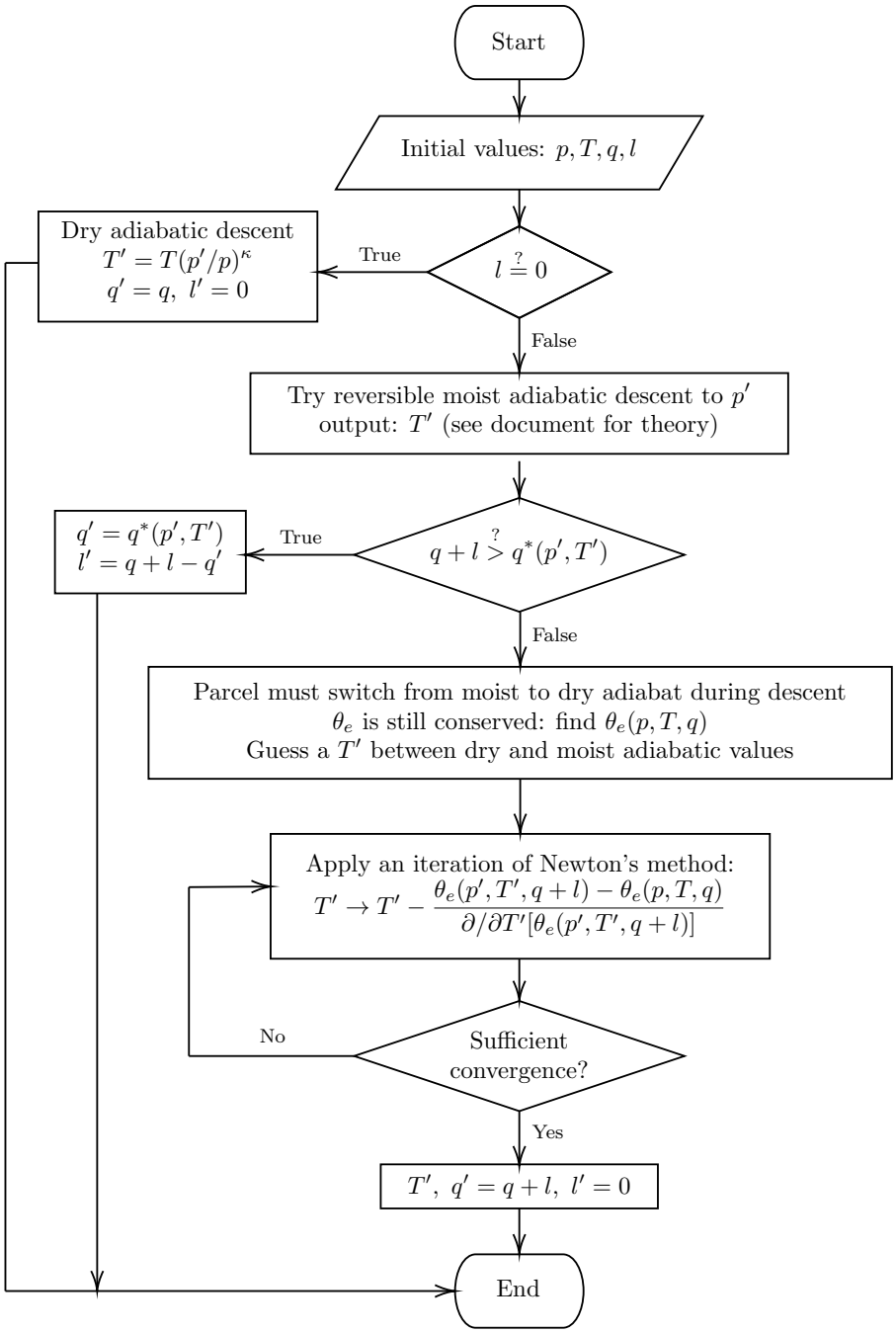

Figure 2: Flowchart for the descent calculation (`descend`) performed at each downward step for the entraining downdraft.

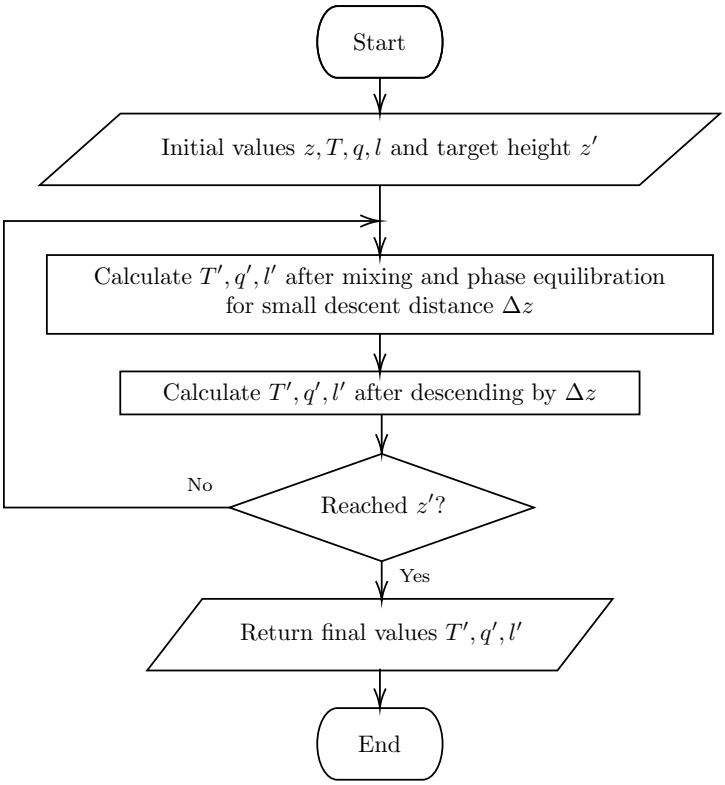

Figure 3: Flowchart for the calculation of parcel temperature as a function of height (`EntrainingParcel.profile`), assembling the routines shown in Figures 1 and 2.

4 Results

The model developed in Section 3 allows for the variation of numerous parameters relevant to downdrafts. One may specify arbitrary initial conditions for height, temperature, specific humidity and liquid water mass ratio, choose the entrainment rate, and use any atmospheric sounding to generate the environmental variables.

4.1 Downdraft initiation and initial conditions

We first envision a downdraft that is initiated by precipitation falling into subsaturated environmental air (the precipitation-associated type identified by Knupp and Cotton (1985)), and investigate the effect of the amount of water evaporated (and the consequent cooling) on downdraft strength and penetration.

An idealised atmospheric sounding is used, with a dry adiabatic temperature profile in a boundary layer near the surface, a capping *inversion* (region of increasing temperature with height) above it, and a moist adiabatic temperature profile in the remaining upper atmosphere, whose relative humidity is constant at 50%. The temperature and dew point profiles in the sounding are depicted in Figure 4. The initial height is set to 5 km, the entrainment rate to $1\,\mathrm{km}^{-1}$ and we test both the case where the initial precipitation does not saturate the parel, and the case where it does, depositing a variable amount of liquid water in addition.

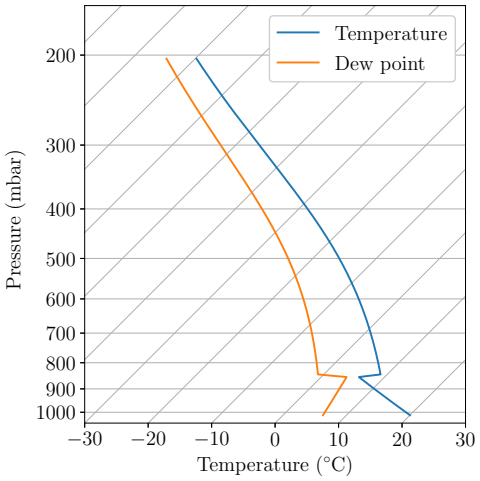

Figure 4: Skew T-log p plot of the idealised atmospheric sounding used in Section 4.1.

Figure 5 shows the height and velocity of the parcels with different sets of initial conditions, and the minimum height and maximum velocity reached as a function of the cumulative amount of water initially added by precipitation. It is clear that both downdraft strength (maximum velocity) and penetration (initial minus final height) are

enhanced by precipitation. This is expected; greater initial evaporation of precipitation reduces the parcel's temperature further, causing it to be more negatively buoyant and to descend further before coming into equilibrium with the environment. The addition of liquid water by precipitation also stregthens these effects, since it contributes to the parcel's weight and allows it to descend moist adiabatically; under this regime, the increase in temperature per unit distance descended is smaller and the parcel again must descend further, and has more time to gain velocity, before coming into equilibrium with the environment.

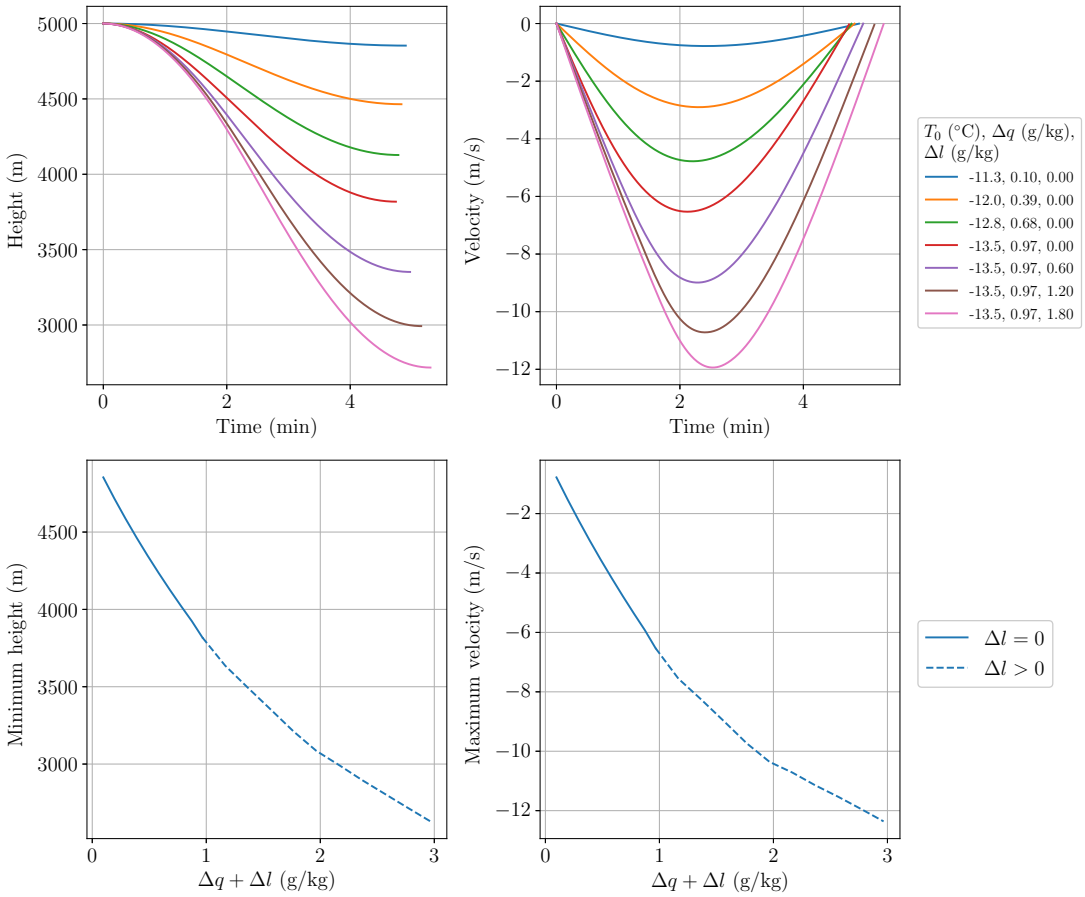

Figure 5: Properties of a downdraft parcel originating at height 5 km in an idealised atmospheric sounding with 50% relative humidity in the upper atmosphere and a fixed entrainment rate of $1\,\mathrm{km}^{-1}$. Top row: height (left) and velocity (right) as functions of time, for selected initial conditions. Bottom row: minimum height reached (left) and maximum downward velocity (right) as functions of the total amount of water initially added to the parcel (specific humidity change due to evaporation Δq plus additional liquid water per unit parcel mass Δl).

4.2 The impact of entrainment

We now investigate the effect of entrainment rate on downdraft strength and penetration. The scenario is similar to the one described in Section 4.1. The initial conditions are fixed: the parcel is initially saturated by precipitation, which deposits $2\,\mathrm{g\,kg^{-1}}$ liquid water in it. The atmospheric sounding used is the same. The entrainment rate is varied between $0\,\mathrm{km^{-1}}$ and $2\,\mathrm{km^{-1}}$, which covers typical measured values (Lu et al. 2016).

Figure 6 depicts the same dependent variables as Figure 5, with the key independent variable now being entrainment rate. We observe that entrainment clearly reduces the strength and penetration of the downdraft; this is attributed to the fact that more vigorous mixing causes the parcel to come into equilibrium with its environment sooner, before it is able to descend as far or gain as much velocity as a parcel experiencing less mixing.

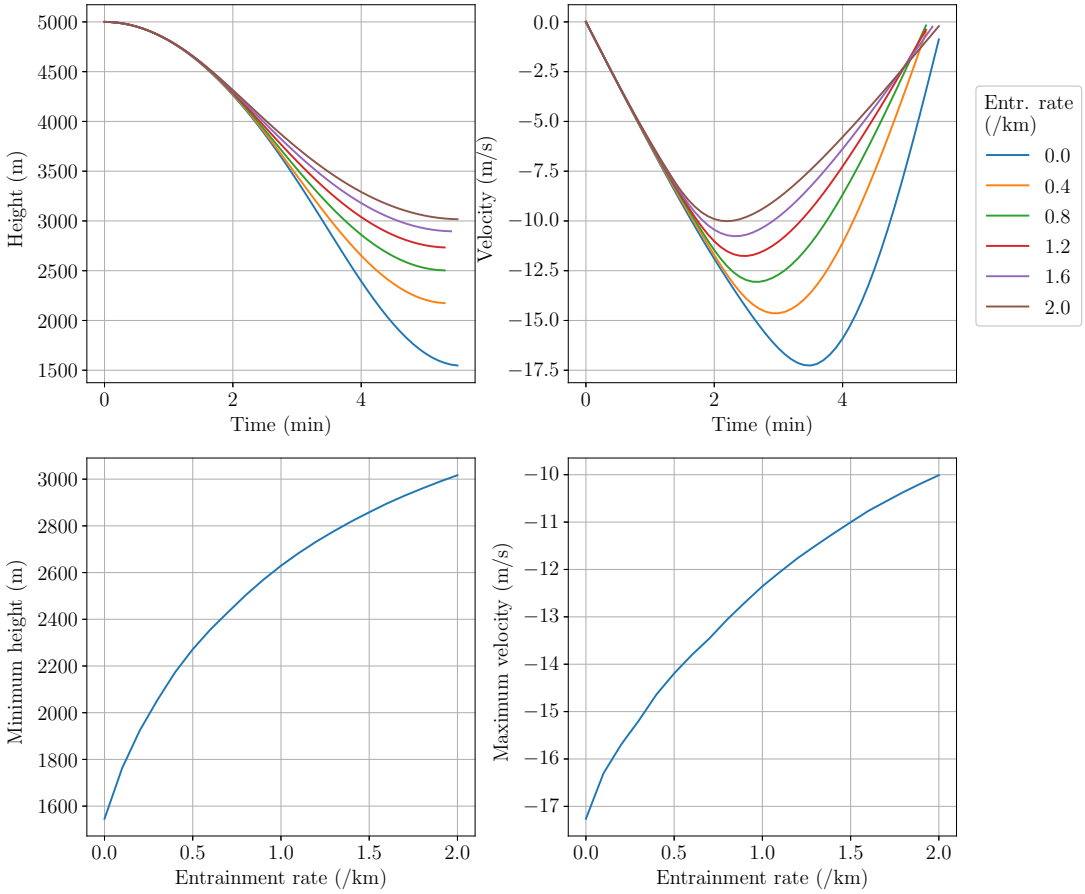

Figure 6: Properties of a downdraft parcel originating at height 5 km in an idealised atmospheric sounding with 50% relative humidity in the upper atmosphere. The initial conditions are fixed: an environmental parcel is brought to saturation by evaporation of liquid water, and $2\,\mathrm{g\,kg^{-1}}$ liquid water is additionally suspended in the parcel. Top row: height and velocity over time for selected entrainment rates. Bottom row: minimum height reached and maximum velocity as functions of entrainment rate.

4.3 The impact of environmental humidity

In the third set of calculations, the environment in which the parcel's motion takes place is varied by changing the relative humidity in the upper part of the idealised sounding described in Section 4.1. The resulting temperature and dew point profiles are shown in Figure 7. The initial conditions are similar to those of Section 4.2: the parcel is initially saturated by precipitation, which deposits $2\,\mathrm{g\,kg^{-1}}$ liquid water in it. However, the varying environmental relative humidity causes the amount of precipitation that may evaporate, and the resulting initial temperature, to vary; in a sounding with lower relative humidity, the parcel experiences more initial evaporation and cooling.

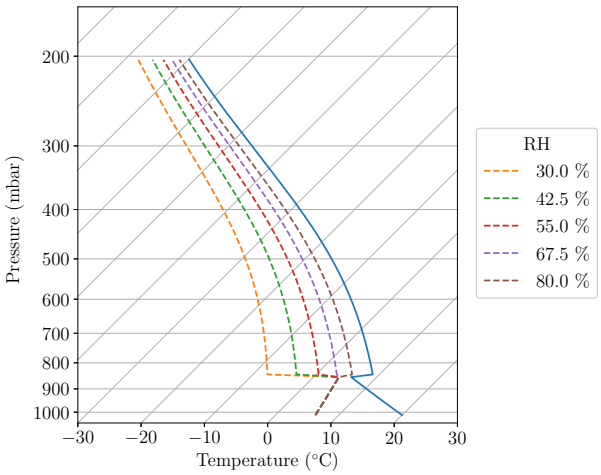

Figure 7: Skew T-log p plot of some selected idealised atmospheric soundings used in Section 4.3. The dashed lines on the left are the dewpoint profiles for the different soundings, and the solid blue line on the right is the common temperature profile.

Figure 8 now depicts the same dependent variables as Figures 5 and 6, with the key independent variable being environmental relative humidity. We observe that the downdraft is stronger and penetrates further in the drier environments due to the greater degree of initial precipitation-induced cooling that is possible, as previously described.

Furthermore, the DCAPE and DCIN were computed for each sounding, allowing the plot of downdraft strength and penetration as functions of these variables shown in Figure 9. The results are in strong agreement with the findings of Market et al. (2017) and Sumrall (2020): the greater the potential energy available and the smaller the inhibition in its way, the further and faster the parcel descends. We also note that, as postulated by Sumrall (2020), smaller ratios of |DCAPE/DCIN| are strongly correlated with increased downdraft strength and penetration.

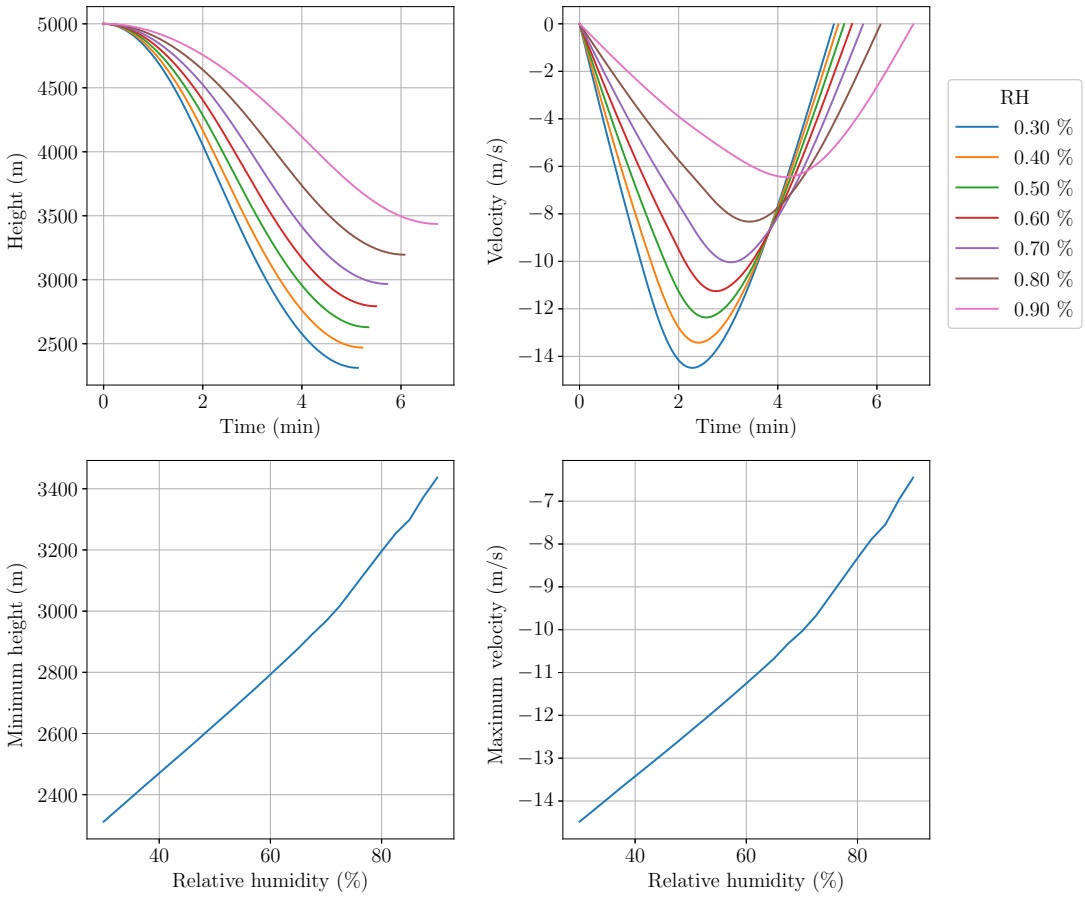

Figure 8: Properties of a downdraft parcel originating at height 5 km in idealised atmospheric soundings whose upper atmosphere relative humidities vary between 30% and 90%. The initial conditions are generated by bringing an environmental parcel to saturation by evaporation of liquid water (note that the resulting temperatures differ since more humid environmental parcels are closer to their wet bulb temperatures), and $2\,\mathrm{g\,kg^{-1}}$ liquid water is additionally suspended in the parcel. Top row: height and velocity of the parcel over time for selected soundings. Bottom row: minimum height reached and maximum downward velocity as functions of relative humidity in the upper atmosphere.

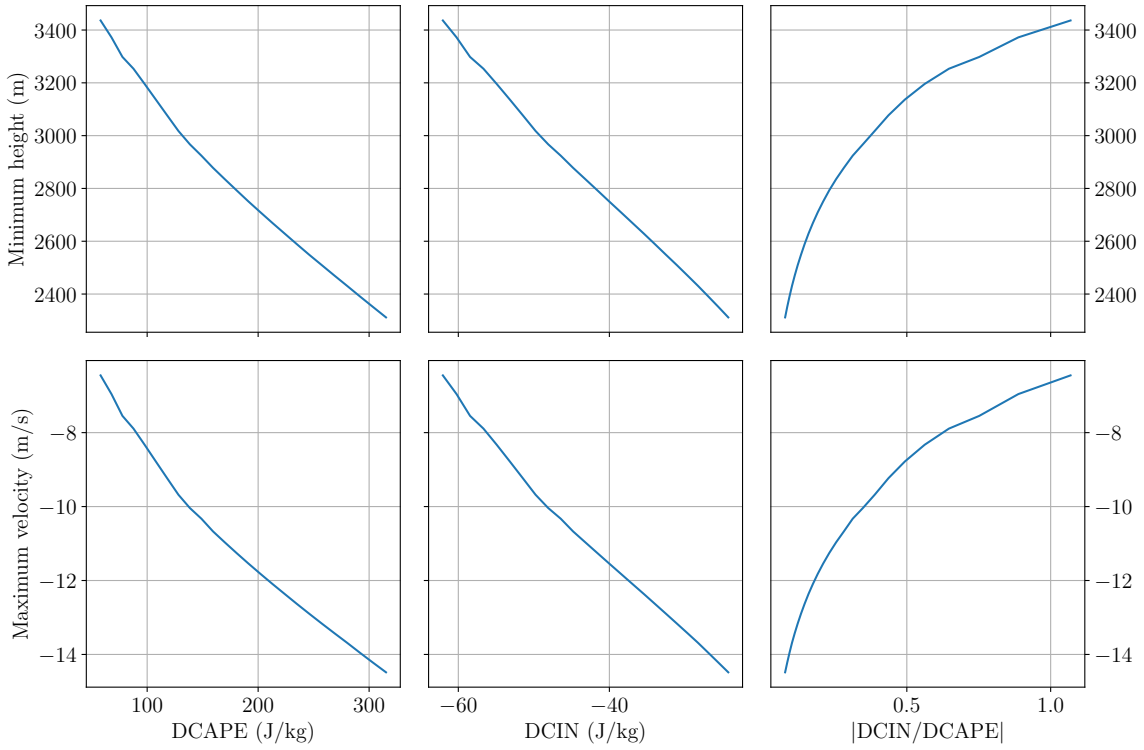

Figure 9: Plots of the minimum height (top row) and maximum downward velocity (bottom row) reached by the parcel of Figure 8 as functions of the downdraft convective available potential energy (DCAPE, left column), downdraft convective inhibition (DCIN, centre column) and the ratio |DCIN/DCAPE| (right column).

5 Conclusions

The construction and testing of a simplified downdraft model, using parcel theory with modifications for entrainment, was highly successful in reproducing the behaviour documented in literature.

There is strong evidence that evaporation of precipitation initiates downdrafts, consistent with the precipitation-associated downdraft type identified by Knupp and Cotton (1985), with the amount of evaporation and liquid water deposited correlating positively with downdraft strength (measured by maximum downward velocity) and penetration (measured by the minimum height reached). We may draw the logical conclusion that downdrafts are stronger, more prevalent and potentially more damaging during storms with heavy precipitation.

It is also observed that the entrainment of environmental air into a downdraft impedes its motion. If it is true that the entrainment rate is inversely proportional to cloud radius (Knupp and Cotton 1985), we may conclude that larger clouds, with smaller entrainment rates, should typically produce stronger, potentially more damaging downdrafts.

It is finally seen that dryness in the atmosphere above the boundary layer allows and maintains stronger downdrafts. Larger values of DCAPE, and smaller values of DCIN and |DCIN/DCAPE|, are associated with stronger and deeper penetrating downdrafts, in excellent agreement with the findings of Market et al. (2017) and Sumrall (2020).

While the simplicity of the model, especially the assumption that no forces other than buoyancy act on parcels, limit the validity of the numerical values generated, it is nevertheless able to unambiguously show the important features of downdraft dynamics in relative terms. Given its simplicity and ease of use, one proposed use for the model is as a supplement to the basic techniques of sounding analysis (such as DCAPE and DCIN calculations) commonly used in weather forecasting. It could be used to estimate the potential for damaging downdrafts based on real atmospheric sounding data within minutes of the data being collected.

Further work may seek to determine which forces other than buoyancy, such as drag, can be incorporated into the model to improve the accuracy and validity of its numerical results without excessive complication and redesigning of the underlying code. A more advanced model might also seek to account for more advanced downdraft dynamics, such as entrainment from an adjacent updraft with momentum transfer in addition to heat and water.

References

Bolton, David (1980). "The computation of equivalent potential temperature". In: *Mon. Weather Rev.* 108.7, pp. 1046–1053. ISSN: 0027-0644.

Davies-Jones, Robert (2008). "An efficient and accurate method for computing the wet-bulb temperature along pseudoadiabats". In: *Mon. Weather Rev.* 136.7, pp. 2764–2785. ISSN: 0027-0644. DOI: 10.1175/2007MWR2224.1.

Knupp, Kevin R and William R Cotton (1985). "Convective cloud downdraft structure: An interpretive survey". In: *Rev. Geophys.* 23.2, pp. 183–215. ISSN: 8755-1209. DOI: 10.1029/RG023i002p00183.

Lu, Chunsong, Yangang Liu, Guang J. Zhang, Xianghua Wu, Satoshi Endo, Le Cao, and Xiaohao Guo (2016). "Improving Parameterization of Entrainment Rate for Shallow Convection with Aircraft Measurements and Large-Eddy Simulation". In: *Journal of the atmospheric sciences* 73.2, pp. 761–773. ISSN: 0022-4928.

Market, P. S, S. M Rochette, J Shewchuk, R Difani, J. S Kastman, C. B Henson, and N. I Fox (2017). "Evaluating elevated convection with the downdraft convective inhibition". In: *Atmos. Sci. Lett.* 18.2, pp. 76–81. ISSN: 1530-261X. DOI: 10.1002/asl.727.

May, Ryan M., Sean C. Arms, Patrick Marsh, Eric Bruning, John R. Leeman, Kevin Goebbert, Jonathan E. Thielen, Zachary S Bruick, and M. Drew. Camron (2021). *MetPy: A Python Package for Meteorological Data*. Version 1.1.0. Unidata. DOI: 10.5065/D6WW7G29. URL: https://github.com/Unidata/MetPy.

Romps, David M (2017). "Exact expression for the lifting condensation level". In: *J. Atmos. Sci.* 74.12, pp. 3891–3900. ISSN: 0022-4928. DOI: 10.1175/JAS-D-17-0102.1.

Saunders, P. M (1957). "The thermodynamics of saturated air: a contribution to the classical theory". In: *Q. J. Roy. Meteror. Soc.* 83.357, pp. 342–350. ISSN: 0035-9009.

Sumrall, Paula (2020). "Using DCIN and DCAPE to evaluate severe surface winds in the case of elevated convection". masters thesis. University of Missouri.

Thayer-Calder, Katherine (2013). "Downdraft impacts on tropical convection". PhD thesis. Colorado State University.